ELSEVIER

Chemical Engineering Journal 76 (2000) 169–177

Chemical Engineering Journal

www.elsevier.com/locate/cej

Transient analysis of isothermal gas flow in pipeline network

S.L. Ke, H.C. Ti *

Department of Chemical and Environmental Engineering, National University of Singapore, Singapore

Received 11 January 1999; received in revised form 6 September 1999; accepted 21 September 1999

Abstract

Conventional methods for transient analysis of pipeline network are normally applied to find the numerical solution of the two partial differential equations (continuity and momentum), which are complex and cumbersome. Following the success of the steady state analysis of pipeline network, this study extends the usage of the electrical analogy method by combining resistance with the theoretically derived models of capacitance and inductance. This method leads to a set of first-order ordinary differential equations for transient analysis of isothermal gas flows in pipeline network. Solving the proposed first-order ordinary differential equation is definitely much simpler than solving the set of partial differential equations. The computational advantages of the present method are demonstrated by comparing them with the conventional methods when applied to a range of pipe network simulation examples. ©2000 Elsevier Science S.A. All rights reserved.

Keywords: Electrical analogy; Gas pipeline; Capacitance, inductance and resistance; Steady and transient analysis; Isothermal flows

1. Introduction

The analysis of flows and pressure drops in piping systems has been studied by many workers and is usually based upon the consideration of steady state conditions. However, the steady state analysis of pipeline network is less applicable, in the design of actual transmission systems, as unsteady (transient) state is more often encountered.

The analysis of unsteady state is much more difficult than that of steady state. The reason for this difficulty is that the unsteady state system is typified by variables which are functions of time and space (or position). In contrast, for steady state analysis, the variable in the system is only a function of space. The introduction of the concept of time variable adds on a new dimension to the mathematical model of the transient flow in a pipe distribution system, and results in computational difficulty. The mathematical model of pipe distribution system is derived from the two conservation equations (mass and momentum), which have the following forms [8]:

$$\frac{\partial \rho}{\partial t}+\frac{\partial(\rho v)}{\partial x}=0 \tag{1a}$$

$$\frac{\partial(\rho v)}{\partial t}+\frac{\partial(\rho v^2)}{\partial x}+\frac{\partial P}{\partial x}+2\rho v^2\left[\frac{\varphi_{\mathrm{f}}}{D}\right]+\rho g\sin\theta=0 \tag{1b}$$

In which ρ is the fluid density, $v(x, t)$ the fluid velocity, $P(x, t)$ is the pressure, φ_{f} is Fanning friction factor, D is the pipe diameter, g is the gravitational acceleration constant, and θ is the angle between the horizon and the longitudinal direction of the pipe.

Many algorithms such as finite difference methods or method of characteristic (MOC) have been used to solve the above partial differential equations [1,8,13]. These methods have been shown to be efficient in solving unsteady flow equations. However, it is not the objective of the present study to follow the conventional route for the analysis of transient flow in pipe distribution system, but to apply electrical analogies to simulate the same transient flow problem.

2. Electrical analogy

The analogy between fluid network and electrical network has been successfully applied in the simulation of steady state pipeline networks by many workers [2,3,11]. From the electrical circuit theory, the three basic elements which relate to voltage and current are viz. resistance, capacitance and inductance. Based on the analogy of voltage and current in an electrical circuit network with that of pressure drop and flow in the fluid network, all the three basic elements should also be present in the fluid distribution systems [5–7,10].

The resistance effect of a pipeline, which has been studied in the steady state analysis of pipeline network, is due to

* Corresponding author. Fax: +65-779-1936
E-mail address: chetihc@nus.eng.sg (H.C. Ti)

1385-8947/00/$ – see front matter
PII: S1385-8947(99)00122-9

several factors, such as the roughness and geometric properties of a pipe, the viscosity of the fluid and the flow rate. The capacitance effect of a pipeline can be directly attributed to the compressibility of the fluid. The inductance effect of a pipeline is believed to be due to the kinetic energy of the fluid [12].

3. Derivation of models for basic elements

The models of resistance and capacitance have been introduced in a previous work [10]. However, it is intended that the models of the three basic elements be derived from Eqs. (1a) and (1b) directly, such that the formulation of the models is explicated theoretically.

Due to pressure change involved in a transient process, the control volume may be compressed or expanded, so the Continuity equation, that is Eq. (1a), can be changed to the following form [1]:

$$\frac{\partial P}{\partial t} + v\frac{\partial P}{\partial x} + \rho a^2 \frac{\partial v}{\partial x} = 0 \tag{2}$$

where a is the acoustical wave velocity.

The Momentum equation, that is Eq. (1b), may be rearranged by multiplying A, the cross-sectional area of pipe to give

$$\frac{\partial(\rho v A)}{\partial t} + \frac{\partial(\rho v A v)}{\partial x} + \frac{\partial(PA)}{\partial x} + 2\rho A v^2\left[\frac{\varphi_f}{D}\right] + \rho A g \sin\theta = 0$$

The first two terms of the above may be expanded as follows:

$$\frac{\partial(\rho v A)}{\partial t} + \frac{\partial(\rho v A v)}{\partial x} = v\frac{\partial(\rho A)}{\partial t} + \rho A\frac{\partial v}{\partial t} + v\frac{\partial(\rho v A)}{\partial x} + \rho v A\frac{\partial(v)}{\partial x}$$

or

$$\frac{\partial(\rho v A)}{\partial t} + \frac{\partial(\rho v A v)}{\partial x} = v\left[\frac{\partial(\rho A)}{\partial t} + \frac{\partial(\rho v A)}{\partial x}\right] + \rho A\frac{\partial v}{\partial t} + \rho v A\frac{\partial(v)}{\partial x}$$

From the Continuity equation Eq. (1a), the term in bracket vanishes; therefore, the Momentum equation becomes

$$\rho\frac{\partial(vA)}{\partial t} + \rho v\frac{\partial(vA)}{\partial x} + \frac{\partial(PA)}{\partial x} + 2\rho A v^2\left[\frac{\varphi_f}{D}\right] + \rho A g \sin\theta = 0 \tag{3}$$

In most engineering applications, the convective acceleration terms, $v[\partial v/\partial x]$; $v[\partial P/\partial x]$ and the slope term are very small compared to the other terms in the above equations and may be neglected [1]. After dropping these terms from Eqs. (2) and (3), the following are obtained:

$$\frac{\partial P}{\partial t} + \rho a^2\frac{\partial v}{\partial x} = 0 \tag{4}$$

$$\frac{\partial(\rho v)}{\partial t} + \frac{\partial P}{\partial x} + 2\rho v^2\left[\frac{\varphi_f}{D}\right] = 0 \tag{5}$$

The discharge Q may be written as

$$Q = vA \tag{6}$$

Substituting Eq. (6) into Eqs. (4) and (5) gives

$$\frac{\partial P}{\partial t} + \frac{\rho a^2}{A}\frac{\partial Q}{\partial x} = 0 \tag{7}$$

$$\frac{\partial Q}{\partial t} + \frac{A}{\rho}\frac{\partial P}{\partial x} + \frac{2\varphi_f Q|Q|}{DA} = 0 \tag{8}$$

Rearranging Eqs. (7) and (8), transient flow through the horizontal pipe can be represented by the following set of equations:

$$\frac{\partial Q}{\partial x} = -\frac{A}{\rho a^2}\frac{\partial P}{\partial t} \tag{9}$$

$$\frac{\partial P}{\partial x} = -\frac{\rho}{A}\frac{\partial Q}{\partial t} - \frac{2\varphi_f \rho Q|Q|}{DA^2} \tag{10}$$

Taking into account that

$$\text{Mass flow rate} = \rho Q = \rho_n Q_n$$

where the subscript n refers to quantities at standard conditions of pressure $P_n \cong 0.1$ MPa and temperature $T_n = 288$ K.

The governing equations become

$$\frac{\partial Q_n}{\partial x} = -\frac{A}{\rho_n a^2}\frac{\partial P}{\partial t} \tag{11}$$

$$\frac{\partial P}{\partial x} = -\frac{\rho_n}{A}\frac{\partial Q_n}{\partial t} - \frac{2\varphi_f \rho_n Q_n|Q|}{DA^2} \tag{12}$$

Based on Eq. (11), we obtain

$$Q_n(x,t) - Q_n(x+\Delta x, t) = Q_C = -\frac{\partial Q_n}{\partial x}\Delta x = \left[\frac{A\Delta x}{\rho_n a^2}\right]\left[\frac{\partial P}{\partial t}\right] \tag{13}$$

where Q_C is the change in flow rate in a pipe dependent on compressibility of the fluid.

Therefore, for the consideration of capacitance effect in a pipeline network, the relationship between pressure and flow rate with capacitance can be made analogous to voltage and current relationship across an electric capacitor in the following form:

Nodal approach $$J = G\frac{dV}{dt} \tag{14}$$

Mesh approach $$V = \frac{1}{G}\int J\,dt \tag{15}$$

where G is the capacitance, reflecting the capacitance effect in a pipeline. Comparing Eq. (14) with Eq. (13), the capacitance has the following form:

$$G = \frac{A\Delta x}{\rho_n a^2} = \frac{V_p}{\rho_n a^2} \tag{16}$$

where V_p is the volume within the pipe.

For gas distributing system under isothermal conditions, we can write the equation of state in the form [8]

$$a^2 = \frac{P}{\rho} = \frac{zR_gT}{MW} \tag{17}$$

Substituting Eq. (17) into Eq. (16), we get

$$G = \frac{V_p\,MW}{\rho_n z R_g T} \tag{18}$$

Similarly, from Eq. (12), we obtain

$$P(x,t) - P(x+\Delta x, t) = -\Delta P = -\frac{\partial P}{\partial x}\Delta x = \frac{\rho_n \Delta x}{A}\frac{\partial Q_n}{\partial t} + \frac{2\varphi_f \rho_n Q_n |Q| \Delta x}{DA^2} \tag{19}$$

We assume

$$-\Delta P_L = \frac{\rho_n \Delta x}{A}\frac{\partial Q_n}{\partial t} \tag{20}$$

and

$$-\Delta P_R = \frac{2\varphi_f \rho_n Q_n |Q| \Delta x}{DA^2} \tag{21}$$

where $(-\Delta P_L)$ is the pressure drop required to accelerate a given mass of fluid [6], which is due to inductance effect and is proportional to the rate of change of flow; and $(-\Delta P_R)$ is the pressure drop due to frictional resistance to flow. It is noted that Eq. (21) is the same as the Darcy–Weisbach formula. Therefore, the total pressure drop of a pipe is the sum of the pressure drop due to resistance effect and the pressure drop due to inductance effect across the pipe.

For the inductance effect in a pipeline network, based on Eq. (20) and the analogy between electrical and hydraulic flow, the analogous relationships for inductance relating to pressure drop and flow rate have the following forms, which are analogous to voltage and current relationship across an electric inductor:

Mesh approach $$V = L\frac{dJ}{dt} \tag{22}$$

Nodal approach $$J = \frac{1}{L}\int V\,dt \tag{23}$$

where L is the inductance, reflecting the inductance effect in a pipe. Comparing Eq. (22) with Eq. (20), the inductance has the following form:

$$L = \frac{\rho_n \Delta x}{A} \tag{24}$$

The mathematical representation of the resistance effect in a pipeline network has been employed in the steady state analysis. The adaptability of this model has already been demonstrated by many workers [2,3,10,11]. It can be expressed either in the forms of impedance *Z* or admittance *Y*, which correspond to the mesh or nodal approach. The relationship between the resistance with the pressure drop and flow rate is analogous to the Ohm's law and can be represented by the following equations:

Mesh approach $$V = ZJ \tag{25}$$

Nodal approach $$J = YV \tag{26}$$

The mathematical model for resistance in a pipeline network depends on the various equations describing the friction factor relationship between pressure drop and flow rate. Weymouth equation has been used in the previous work [10] on Osiadacz's sample networks [8]. Other equations used in the present study are listed as follows [8]:

Lacey's equation — (for the pressure range of 0–75 mbar gauge):

$$\varphi_f = 0.0044\left[1 + \frac{12}{0.276D}\right] \tag{27a}$$

The Polyflo equation — (for the pressure range of 0.75–7.0 bar gauge):

$$\sqrt{\frac{1}{\varphi_f}} = 5.338Re^{0.076}\eta \tag{27b}$$

The Panhandle 'A' equation — (for the pressure range above 7.0 bar gauge):

$$\sqrt{\frac{1}{\varphi_f}} = 6.872Re^{0.073}\eta \tag{27c}$$

where η is the efficiency factor accounting for the additional frictional or drag losses other than losses due to viscous forces.

4. Derivation of equations for the transformation approach

In order to derive the mathematical model for transient flow analysis, some of the fundamental assumptions used in the conventional methods are also applied. These assumptions are (i) one-dimensional and isothermal flow, and (ii) applying the steady state friction factor equation to transient flow [1,8].

As mentioned above, the change of flow rate across a pipe with time is due to compressibility of the fluid, i.e. the capacitance effect. The pressure drop of a pipe is the sum of the pressure drop due to resistance effect and the pressure drop due to inductance effect across the pipe. A typical branch of fluid network with transient flow can be represented as an electrical circuit and be visualised in Fig. 1. The resistance and inductance are proposed to be connected in series, and the capacitance and resistance are proposed to be connected in parallel.

Based on Fig. 1, the following relationships can be drawn:

$$V = V_1 + V_2 \tag{28}$$

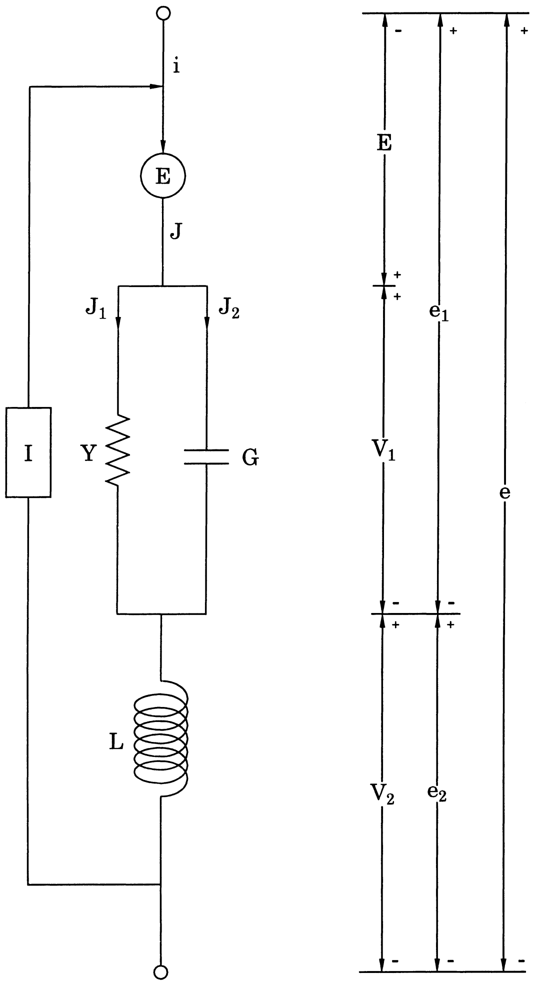

Fig. 1. Composite branch of a network.

$$V_1 = E + e_1 \quad (29)$$

$$V_2 = e_2 \quad (30)$$

$$J = I + i \quad (31)$$

$$J = J_1 + J_2 \quad (32)$$

For the nodal approach [14]

$$J_1^{b} = Y^{bb} V_{1b} \quad (33)$$

$$J_2^{b} = G^{bb} \frac{dV_{1b}}{dt} \quad (34)$$

Based on Eq. (22),

$$V_{2b} = L_{bb} \frac{dJ^{b}}{dt} \quad (35)$$

Applying the transformation theory [14],

$$J^{s} = A^{s}_{\cdot b} J^{b} = A^{s}_{\cdot b}(J_1^{b} + J_2^{b}) = A^{s}_{\cdot b}\left[Y^{bb} V_{1b} + G^{bb}\frac{dV_{1b}}{dt}\right] \quad (36)$$

$$V_{2s} = C_{s}^{\cdot b} L_{bb} C^{b}_{\cdot s} \frac{dJ^{s}}{dt} \quad (37)$$

Substituting

$$V_{1b} = A_{b}^{\cdot s} V_{1s} \quad (38)$$

into Eq. (36), the following equation is obtained:

$$\begin{aligned} J^{s} &= A^{s}_{\cdot b}\left[Y^{bb} A_{b}^{\cdot s} V_{1s} + G^{bb} A_{b}^{\cdot s} \frac{dV_{1s}}{dt}\right] \\ &= A^{s}_{\cdot b} Y^{bb} A_{b}^{\cdot s} V_{1s} + A^{s}_{\cdot b} G^{bb} A_{b}^{\cdot s} \frac{dV_{1s}}{dt} \end{aligned} \quad (39)$$

When Eqs. (39) and (37) are extended to open path and closed path frameworks, they become

$$\begin{aligned} \left[\frac{J^{o}}{J^{c}}\right] &= \left[\frac{A^{o}_{\cdot b}}{A^{c}_{\cdot b}}\right] Y^{bb}[A_{b}^{\cdot o} | A_{b}^{\cdot c}] \left[\frac{V_{1o}}{V_{1c}}\right] \\ &\quad + \left[\frac{A^{o}_{\cdot b}}{A^{c}_{\cdot b}}\right] G^{bb}[A_{b}^{\cdot o} | A_{b}^{\cdot c}] \left[\frac{dV_{1o}/dt}{dV_{1c}/dt}\right] \end{aligned} \quad (40)$$

$$\left[\frac{V_{2o}}{V_{2c}}\right] = \left[\frac{C_{o}^{\cdot b}}{C_{c}^{\cdot b}}\right] L_{bb}[C^{b}_{\cdot o} | C^{b}_{\cdot c}] \left[\frac{dJ^{o}/dt}{dJ^{c}/dt}\right] \quad (41)$$

As

$$V_{1o} = E_{o} + e_{1o} = C_{o}^{\cdot b} E_{b} + e_{1o} \quad (42)$$

$$V_{1c} = E_{c} = C_{c}^{\cdot b} E_{b} \quad (43)$$

for an invariant pressure source E_b, we obtain the following relationships:

$$\frac{dV_{1o}}{dt} = \frac{de_{1o}}{dt} \quad (44)$$

$$\frac{dV_{1c}}{dt} = 0 \quad (45)$$

Expanding Eqs. (40) and (41), and incorporating Eqs. (44) and (45), we have

$$\begin{aligned} J^{o} &= A^{o}_{\cdot b} Y^{bb} A_{b}^{\cdot o}(C_{o}^{\cdot b} E_{b} + e_{1o}) + A^{o}_{\cdot b} Y^{bb} A_{b}^{\cdot c} C_{c}^{\cdot b} E_{b} \\ &\quad + A^{o}_{\cdot b} G^{bb} A_{b}^{\cdot o} \frac{de_{1o}}{dt} \end{aligned} \quad (46)$$

$$\begin{aligned} J^{c} &= A^{c}_{\cdot b} Y^{bb} A_{b}^{\cdot o}(C_{o}^{\cdot b} E_{b} + e_{1o}) + A^{c}_{\cdot b} Y^{bb} A_{b}^{\cdot c} C_{c}^{\cdot b} E_{b} \\ &\quad + A^{c}_{\cdot b} G^{bb} A_{b}^{\cdot o} \frac{de_{1o}}{dt} \end{aligned} \quad (47)$$

$$e_{2o} = C_{o}^{\cdot b} L_{bb} C^{b}_{\cdot o} \frac{dJ^{o}}{dt} + C_{o}^{\cdot b} L_{bb} C^{b}_{\cdot c} \frac{dJ^{c}}{dt} \quad (48)$$

Rearranging Eq. (46), we have

$$\begin{aligned} \frac{de_{1o}}{dt} &= [A^{o}_{\cdot b} G^{bb} A_{b}^{\cdot o}]^{-1}[J^{o} - A^{o}_{\cdot b} Y^{bb} A_{b}^{\cdot o}(C_{o}^{\cdot b} E_{b} + e_{1o}) \\ &\quad + A^{o}_{\cdot b} Y^{bb} A_{b}^{\cdot c} C_{c}^{\cdot b} E_{b}] \end{aligned} \quad (49)$$

Eqs. (47) to (49) are the governing equations for transient pipe flow system with a constant pressure source; and they are a set of first-order ordinary differential equations. Hence, the transient pipe flow problem which is ordinarily governed by the set of two partial differential equations can now be solved by a set of first-order ordinary differential equations which is much easier to handle. Nevertheless, these equations can not be solved analytically owing to the complicated relationships involved in the network problem.

For a network with known topology, tensors $A^{o}_{\cdot b}$, $A^{\cdot o}_{b}$, $A^{c}_{\cdot b}$, $A^{\cdot c}_{b}$, $C^{b}_{\cdot o}$, $C^{b}_{\cdot o}$, $C^{b}_{\cdot c}$, and $C^{\cdot b}_{c}$ and inductance are independent of time and can be determined easily; while the boundary condition of admittance and capacitance can be calculated based on the results of steady state analysis. Therefore, the dynamic response of e_{1o} can be determined through the solution of a series of ordinary differential equations as Eq. (49). When e_{1o} is found, J^{c} can be calculated from Eq. (47). Then, e_{2o} is calculated from Eq. (48). Using e_{o} and J^{c}, the dynamic change of branch flow, branch pressure drop and nodal pressure of network at any given time can be found through the application of the transformation techniques.

5. Computational scheme

Once the topology of the pipeline network is ascertained, the steady state analysis of pipeline network can be carried out to find the branch flow rate and nodal pressure, which are then used as the initial value to solve the ordinary differential equation. The steady state analysis of a pipe network can be based either on the mesh method or its dualistic nodal method. Once the steady state analysis is completed, the transient calculation is carried out by using the general solution method such as the fourth-order Runge–Kutta method for the first-order ordinary differential equations. The detailed computation scheme is outlined in Fig. 2. The computer program is written in Microsoft FORTRAN and runs on a Pentium/75 PC.

6. Sample networks

The mathematical model derived in the present study was tested on three simple gas networks, two of which have been analysed by Osiadacz [8] and one by London Research Station (LRS) [4]. The first sample network is a straight pipeline ($l = 10^5$ m) with a uniform diameter of 0.6 m. The upstream pressure is maintained at a constant level of 5 MPa. The flow rate is depicted in Fig. 3. The operating temperature is 278 K; the density of the fluid is 0.73 kg m^{-3}; and the specific gravity of the fluid is 0.6. For the purpose of analysing, the pipeline is cut into five segments. Thus, the capacitance of each segment is five times the capacitance of the pipe. Osiadacz's result is presented in Fig. 4.

The second example is a simple network with three nodes and three branches forming one mesh as shown in Fig. 5. The physical data are shown in Table 1.

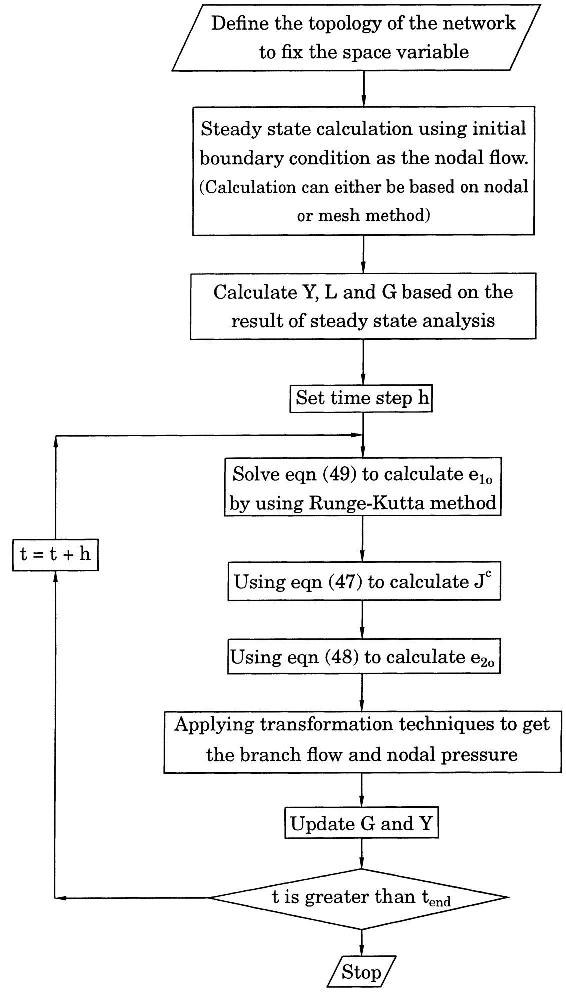

Fig. 2. Computational flow chart.

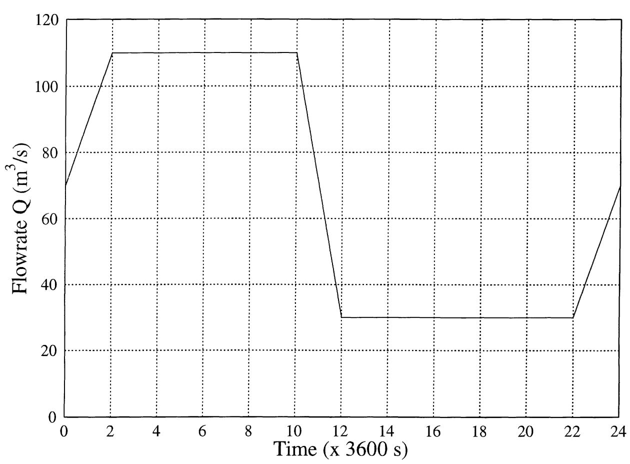

Fig. 3. Change of flow with time (boundary condition).

Node 1 is the pressure source with a constant pressure of 5 MPa. The loads at Nodes 2 and 3 are known functions of time, which vary according to the curves depicted in Fig. 6. In this example, each pipe is cut into four segments. Hence, the capacitance of each segment is equal to the capacitance of the pipe multiplied by 4 [15].

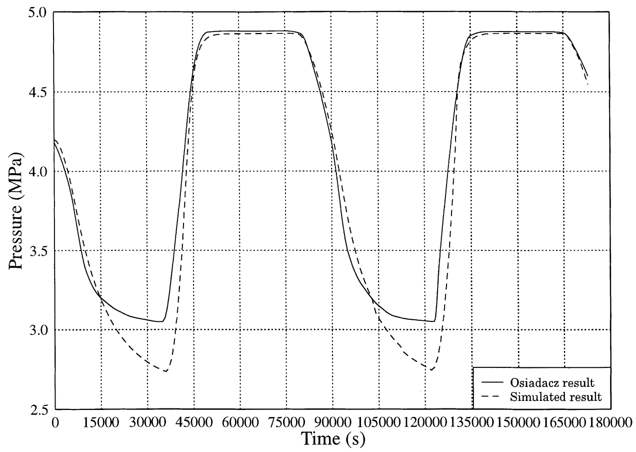

Fig. 4. Change of pressure at the outlet for Sample Network 1.

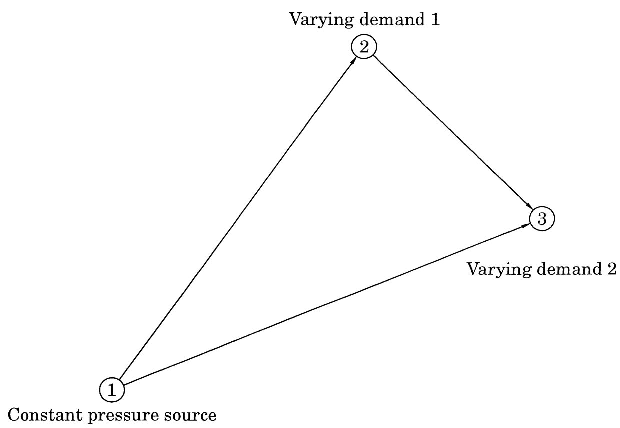

Fig. 5. Sample Network 2.

Table 1
Pipe data of the second sample network[a]

Pipe	From	To	Diameter (m)	Length (m)
1	1	3	0.6	80000
2	1	2	0.6	90000
3	2	3	0.6	100000

[a] $\rho = 0.7165\,\mathrm{kg\,m^{-3}}$; $S = 0.6$; $T = 278\,\mathrm{K}$; $t_{max} = 86{,}400\,\mathrm{s}$.

The last sample network is a straight pipe having a uniform diameter. This sample network was used by LRS in demonstrating the versatility of their program PAN. Initially, the pipe was in a steady state; the demand then increased by 50% in a step change and was held constant thereafter. The pressure at the inlet, P_1, was held constant, while the pressure at the outlet, P_2, fell to a new steady state value. In this case, each pipe is cut into four segments and the capacitance of each segment is four times the capacitance of the pipe. The analysis was carried out for five different pressure ranges which corresponded to typical pressure range for low, medium and high. The operating conditions are listed in Table 2. The LRS results are depicted in Figs. 9–13.

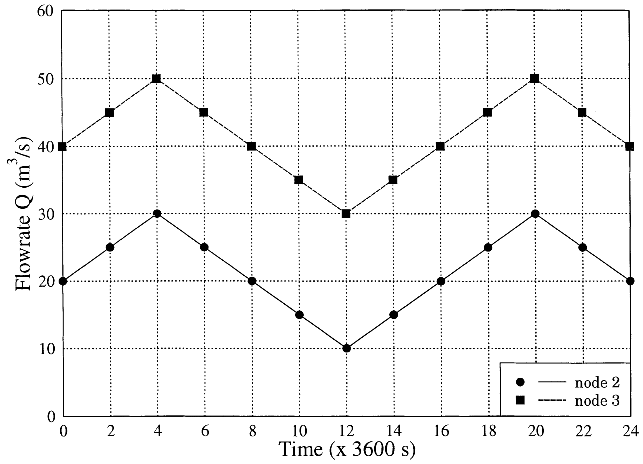

Fig. 6. Changes of load at Nodes 2 and 3 for Sample Network 2.

Table 2
Pipe data of the third sample network

	Length (mile)	Diameter (in.)	Initial flow rate (MSCFH)	Inlet pressure
LRS 1	80	18	1500	350 psig
LRS 2	20	12	800	180 psig
LRS 3	6	14	300	25 psig
LRS 4	3	14	80	2 psig
LRS 5	0.6	4	4	20 in. water gauge

The compressibility factor in this study is determined by using the following correlation:

$$z = \frac{1}{1 + \alpha P_{ave}} \tag{50}$$

where α is obtained from linear interpolation of the constant taken from Gas engineers' Handbook [9] and P_{ave} is the average pressure of each pipe section.

7. Results and discussion

The dynamic pressure response at the outlet of the first sample network as simulated by the derived model is presented in Fig. 4. The computation time spent for solving the examples ranges from approximately 10 s to 5 min, depending on the different time steps used.

Simulation results of the second sample network using the present model is compared with the results from the literature. These are shown in Figs. 7 and 8.

It can be seen that the results obtained by using the present method are comparable with those in the literature. The deviation is less than 9% for the first example and 1% for the second example. When the last sample network was analysed, it was found that the average simulated pressure response was higher than the LRS result by around an average of 10% (the maximum error is around 27% for the case of lowest pressure). This result shows that the response was slower, due to the high value of capacitance. Upon further

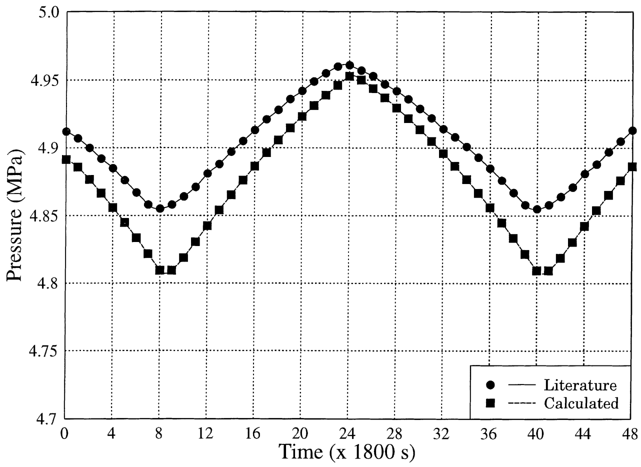

Fig. 7. The variation of pressure at Node 2.

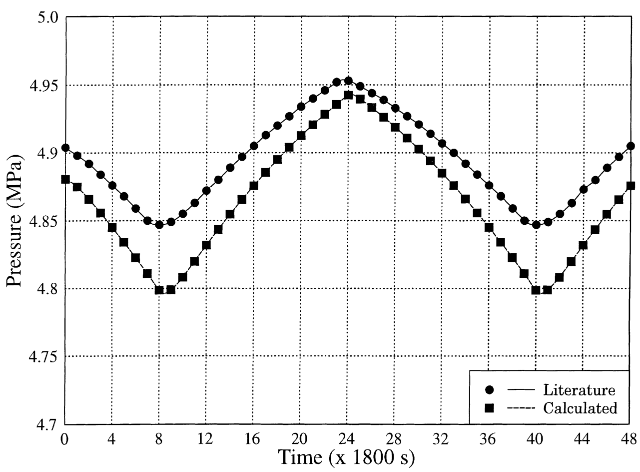

Fig. 8. The variation of pressure at Node 3.

investigation, it was found that, when the temperature was decreased, the capacitance became larger and the response slowed down. As most pipes were buried underground and the pipe wall temperature subjected to daily temperature change, the assumption of isothermal condition made in the derivation of Eq. (18) might not satisfy the LRS conditions. In order to avoid a more complicated model of considering the conservation of energy, an efficiency factor is adopted in the present study to consider the deviation from the assumption of isothermal flow condition. After numerous trials, a factor of 0.65 was selected based on the first case of LRS result ($P_1 = 350$ psig). It was found that the same factor of 0.65 would fit the other four cases of LRS with a maximum error of 7%. The results are depicted in Figs. 9–13.

Convergence is normally a common problem in the analysis of pipeline network. However, in this present study, iteration process is only required in the part of steady state analysis; and the solution of transient analysis can be obtained without any convergence difficulty. Moreover, the steady state analysis was carried out using the robust transformation method [3,11], and hence, convergence problem was manageable.

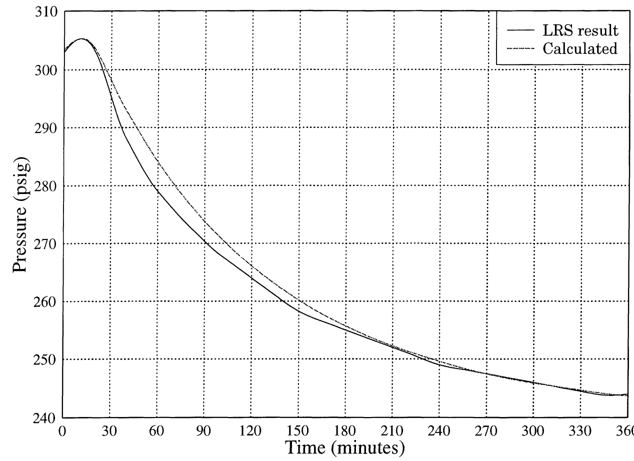

Fig. 9. Comparison of simulated pressure with the LRS result ($P_1 = 350$ psig).

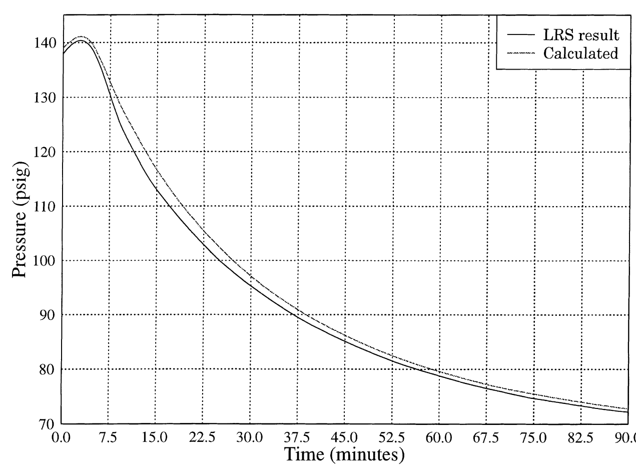

Fig. 10. Comparison of simulated pressure with the LRS result ($P_1 = 180$ psig).

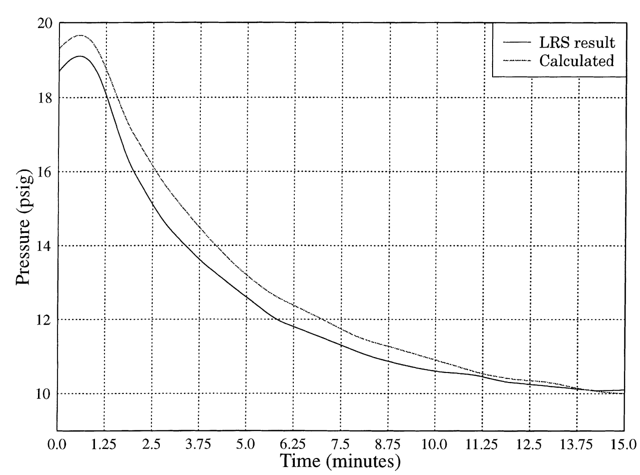

Fig. 11. Comparison of simulated pressure with the LRS result ($P_1 = 25$ psig).

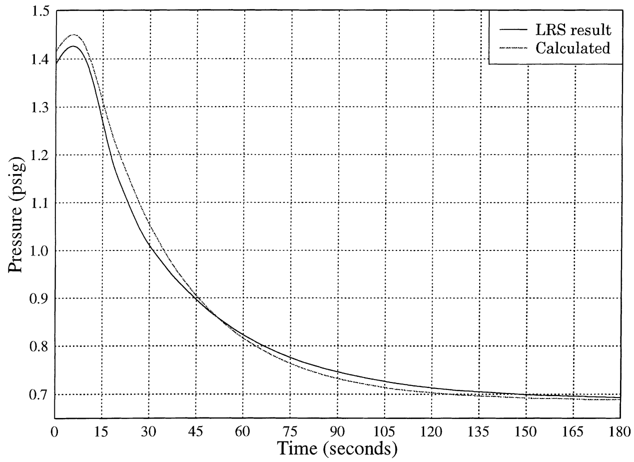

Fig. 12. Comparison of simulated pressure with the LRS result ($P_1 = 2$ psig).

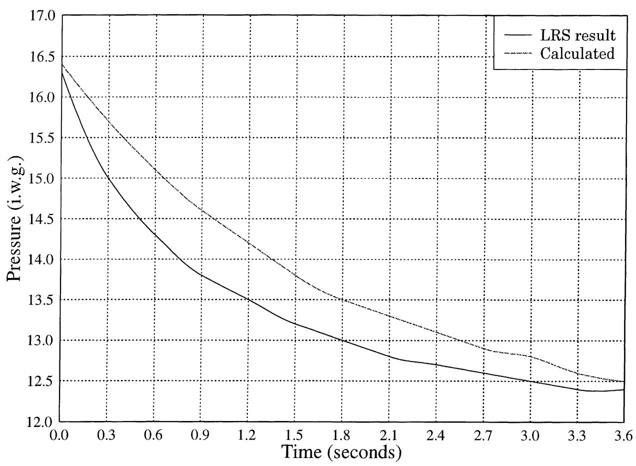

Fig. 13. Comparison of simulated pressure with the LRS result ($P_1 = 20$ i.w.g.).

The present study also investigated the effect of space and time discretization on the accuracy of solution. This is done by comparing the simulation results of the second sample network when all pipes were cut into four and eight equal parts. It is found that discretization of pipe section does not affect the precision of simulation result for the pipe network examined. It is also found that the variation of time step has negligible effect on the simulation result. On the other hand, both space and time discretization have noticeable effect on the computation effort needed, i.e. the finer the space or time steps, the more is the computation time required. For a node with a sudden change of high demand, a smaller time space is recommended.

The inductance effect on the solution of gas transient flow is also investigated. Simulation results of pipe flow with the inductance effect considered were compared to that when inductance effect was neglected. It is found that the effect of inductance which corresponds to kinetic energy of gas is negligible on the simulation results for the gas pipe networks examined compared to the resistance and capacitance effects. Hence, when the boundary conditions of a gas pipeline network do not change rapidly or the capacity of the pipe is relatively large, the effect of inductance can be neglected . Nevertheless, further study on the inductance effect for hydraulic transient analysis is recommended.

8. Conclusion

A new mathematical model based on electrical analogy and transformation theory is developed for transient analysis of isothermal gas flow in pipe networks. The transient behaviour of a pipe, conventionally taking the form of a set of second-order partial differential equations, can be expressed by a set of first-order ordinary differential equations using the new model. The solutions computed using the new method are compatible with those using the conventional methods. The new method is simple, straight forward and without convergence problem. It is easy to implement on a small personal computer. Comparing with the conventional methods, this new method shows a promising feature in saving computational efforts and may be employed as a powerful means for pipe network design and control.

9. Nomenclature

A	transformation tensor or cross-sectional area
C	matrix or transformation tensor used in the mesh approach
D	diameter of a pipe
E	covariant tensor for pressure source across a branch or path
e	covariant tensor for pressure drop across a branch or path
G	contravariant tensor for capacitance used in the nodal approach
I	contravariant tensor for flow due to external input–output on a branch or path
i	contravariant tensor for flow due to other cause on a branch or path
J	contravariant tensor for total flow on a branch or path
L	contravariant tensor for inductance used in the mesh approach
l	length of a pipe
MW	molecular weight of fluid
ΔP	pressure drop across a pipe
P_1, P_2	pressure at the nodes
P_{ave}	average pressure of a pipe
Q_n	volumetric flow rate of fluid at standard state
Re	Reynolds number
R_g	gas constant
S	specific gravity of gas
T	absolute temperature (K)
V	contravariant tensor for pressure drop due to impedance, where $V = E + e$

V_P volume within pipe
v fluid velocity
Y contravariant tensor for admittance used in the nodal approach
Z contravariant tensor for impedance used in the mesh approach
z compressibility factor
η efficiency factor
φ_f Fanning friction factor
ρ density of fluid

9.1. Index symbols

b index used in tensor form, indicating that the tensor is in primitive framework
c index used in tensor form, indicating that the tensor is in closed path framework
o index used in tensor form, indicating that the tensor is in open path framework
s index used in tensor form, indicating that the tensor is in orthogonal framework

References

[1] M.H. Chaudhry, Applied Hydraulic Transients, Van Nostrand Reinhold, New York, 1987.
[2] B. Gay, P. Middleton, The solution of pipe network problems, Chem. Eng. Sci. 26 (1971) 109–123.
[3] B. Gay, P.E. Preece, Matrix methods for the solution of fluid network problems Part I. Mesh methods, Trans. Inst. Chem. Engrs. 53 (1975) 12–15.
[4] London Research Station, Proceedings of PAN Presentation, British Gas Corporation, 27 February 1974.
[5] S.D. Millston, Electric analogies for hydraulic analysis Part 1. System components, Machine Design December (1952) 185–189.
[6] S.D. Millston, Electric analogies for hydraulic analysis Part 2. Tubing characteristics, Machine Design January (1953) 166–170.
[7] G. Murphy, D.J. Shippy, H.L. Luo, Engineering Analogies, Iowa State University Press, IA, 1963.
[8] A.J. Osiadacz, Simulation and Analysis of Gas Networks, E. & F.N. Spon, London, 1987.
[9] C.G. Segeler, M.D. Ringler, E.M. Kafka, Gas Engineers' Handbook, AGA, NY, 1969.
[10] W.Q. Tao, H.C. Ti, Transient analysis of gas pipeline network, Chem. Eng. J. 69 (1997) 47–52.
[11] H.C. Ti, K.G. Koh, H.M. Tar, Steady analysis of gas flow in a pipeline network, in: Proceedings of the 4th Asean Council on Petroleum (ASCOPE) Conference & Exhibition, November 1989, Singapore, pp. 484–489.
[12] J.F. Wilkinson, D.V. Holliday, E.H. Bakey, K.W. Hannah, Transient Flow in Natural Gas Transmission Systems, AGA, NY, 1965.
[13] E.B. Wylie, V.L. Streeter, Fluid Transients, McGraw-Hill, New York, 1978.
[14] G. Kron, Tensor Analysis of Networks, MacDonald, London, 1965.
[15] R.G. Meadows, Electric Network Analysis, The Athlone Press, London, 1972.